Praise Worthy Prize
International Review of Aerospace Engineering (I.RE.AS.E), Vol. 11, N. 4
ISSN 1973-7459 August 2018

Avoiding Local Minima for Path Planning Quadrotor Based on Modified Potential Field

Iswanto

Abstract – *The study aims to present potential field algorithm for quadrotor path planning in an unknown area. There are several problems found in quadrotor path planning including how to reach the goal position quickly, avoid static obstacles and loca minima. To overcome the problem, a modified potential force algorithm was used. Potential field algorithm is an algorithm consisting an attractive force to move the quadrotor to the goal position and repulsive force to avoid obstacles in the area. There are some obstacles with their repulsive force value is equal to their attractive force resulting in no resultant force, and creating a local minima causing the quadrotor stop. Hence, this study presented a modification of the potential field algorithm to be applied in the quadrotor so that the quadrotor can avoid the loca minima. The proposed algorithm was modified by making a virtual obstacle which has a repulsive force so that the resultant force is not equal to zero and no local minima generated.*

Keywords: *Path Planning, Quadrotor, Local Minima, Potential Field, Avoid Obstacles*

Nomenclature

T	Quadrotor thrust
(τ_x)	Thrust to the x-axis
(τ_y)	Thrust to the y-axis
(τ_z)	Z-axis rotation force
U_{art}	Artificial Potential Field (APF)
U_{x_d}	Attractive APF
U_O	Repulsive APF
F_{x_d}	Attractive APF force
F_O	Repulsive APF force
F_{art}	Artificial Potential Field force
k_a	Attractive potential constant
x	Robot position
ξ	Speed booster
$\dot{x}$	Speed
x_d	Goal position
O	Obstacle position
η	Repulsive potential constant
ρ	The closest distance between the robot and the obstacle
ρ_O	Distance limit of the potential field influence
(x_Γ, y_Γ)	Goal position value
ψ	The angle formed by $F_{art\_x}(x,y)$ and $F_{art\_y}(x,y)$
(x_d, y_d)	Goal position
(x_t, y_t)	Robot position
d_l	The closest distance to the goal position
(x_O, y_O)	Obstacle position
d_O	The safest distance to avoid obstacles

I. Introduction

A potential field, a method found by Khatib [1] is an algorithm used to move a robot from the initial position to the goal position by the magnetic attraction and repulsion. The potential field generates the attraction used by Khatib to move the robotic arm to the goal position and repulsion used to drive the robot to avoid obstacles. Potential field algorithm has been studied by several researchers such as Faverjon & Tournassoud who implemented an artificial potential field algorithm to move a robot manipulator [2]. The robots used by the researchers had more than 4 degrees of freedom (dof).

The space between the obstacles should be considered in order for the robots which have many DOFs to move to the goal. The former researchers merely applied Artificial Potential field to some robot models. The potential field force was used to attract the robot to goal position and reject the robot to avoid obstacles. The modification of artificial potential field has been conducted by several researchers for robot path planning.

One of the later researchers, Warren [3], used potential field algorithm with the global view to create robot path planning. The attractive and repulsive forces in artificial potential field were used to make the safest path for the robot. A problem in the potential field algorithm is that

 https://doi.org/10.15866/irease.v11i4.14438

the local minima generated by the obstacles due to the sum of attraction and repulsion value of the obstacles is zero causing the robot to stop at the loca minima. Several researchers have conducted research to address such problems including Connolly et al. [4] who modified potential field using Laplace equation. The equation creates a harmonic function changing the potential field into the harmonic potential field. By using the harmonic potential field to avoid loca minima, the robot was able to avoid obstacles.

Barraquand et al. [5] modified potential field to avoid loca minima by adding numerical calculations resulting in w-potential and c-potential algorithms. The modification was called numeric potential field technique, and with such technique the robot was able to avoid local minima. Xiaoping Yun & Ko-Cheng Tan [6] modified potential field algorithm by adding wall following algorithm to avoid loca minima. When the robot is at the point of loca minima, it will use the wall following algorithm to escape from the local minima.

Newman & Hogan [7] modified the potential field and potential dynamic function. They used the algorithm modification to move robot manipulator to reach the goal and avoid obstacles. By modifying the potential field and the dynamics potential function, the robot manipulator can be controlled quickly to avoid obstacles. Kim & Khosla modified Harmonic potential field by adding some laplace equations [8]. By using harmonic potential field modification, the robot was able to avoid obstacles in real time. The potential field algorithm was modified by converting it into potential field virtual force and then the force was applied to kinematic robot model. This research was conducted by Borenstein & Koren [9]. The potential field force is the resultant of attractive and repulsive forces which has a direction. The force affects the mobile robot acceleration. The resultant force is changed into the acceleration to move the robot, while the direction of the force is used to direct the robot.

The potential field algorithm was modified by Spence & Hutchinson [10] to avoid dynamic obstacles. The modification was called Integrating Potential field using dynamic inverse control. By modifying the repulsive force of the potential field, the robot was able to avoid the obstacles.

The other researcher, Sundar & Shiller [11] modified potential field by using Hamilton-Jacobi-Bellman equation. The equation was used to make closer the distance between the robot and the obstacles when the robot was escaping from the obstacles so that the distance between the robot to the goal position would be closer.

Masoud et al. [12] modified harmonic potential into a bi-harmonic potential used for wheeled robot navigation to avoid obstacles and reach the goal

Dozier et al. [13] modified potential field by combining potential field algorithm, genetic algorithm, and hill climbing algorithms. The combination of these three algorithms was used to detect static and dynamic obstacles. The algorithm was applied in a wheeled robot navigation to avoid dynamic and static obstacles and reach the goal position.

Zhu et al. [14] modified potential field by combining potential field algorithm, wall following algorithm. The combination of these two algorithms was used to detect polygonal obstacles. The algorithm was applied in wheeled robot navigation to avoid polygonal obstacles and reach the goal position. To avoid local minima, this paper presents a modified potential field algorithm using a virtual obstacle applied in a quadrotor path planning.

II. Artificial Potential Field Algorithm

Potential field is one of the path planning algorithms with magnetic attraction and repulsion methods found by Khatib [1] as it is shown in Fig. 1. It can be seen that x_d is the goal position, x is the robot position, F_{x_d} is the Attractive APF, O is the obstacle position, and F_O is the Repulsive APF [15].

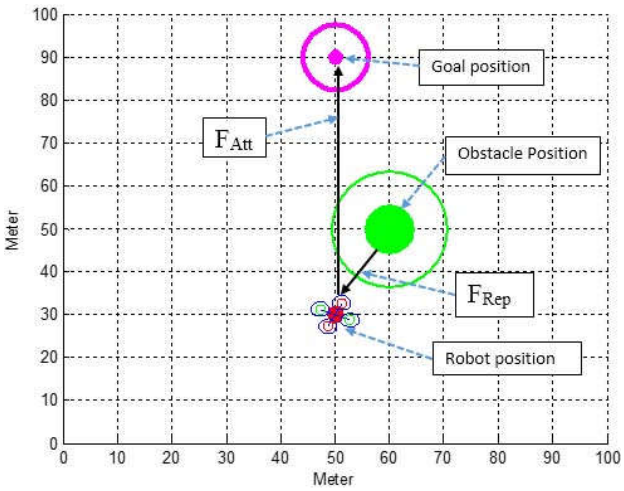

Fig. 1. Artificial potential field model

This algorithm has the value resulted by the sum of repulsive and attractive forces as shown in the following equation [1]:

$$U_{art} = U_{x_d} + U_O \tag{1}$$

where U_{art} is the Artificial Potential field (APF), U_{x_d} is the Attractive APF, and U_O is the Repulsive APF. The following is the APF force equation:

$$F_{art} = F_{x_d} + F_O \tag{2}$$

where F_{x_d} is the attractive APF force and F_O is the repulsive APF force. The attractive APF and the repulsive APF equations are as follows:

$$F_{x_d} = -\text{grad}\left[U_{x_d}\right] \tag{3}$$

$$F_O = -\text{grad}\left[U_O\right] \tag{4}$$

The attractive APF U_{x_d} equation is as follows:

$$U_{x_d} = \frac{1}{2} k_a \left(x - x_d\right)^2 \tag{5}$$

where k_a is the attractive potential constant and x is the robot position.

Thus, the Khatib's attractive APF force equation is:

$$F_{x_d} = -k_a \left(x - x_d\right) - \xi \dot{x} \tag{6}$$

where ξ is the speed booster and $\dot{x}$ is the speed.

The Repulsive APF Equation U_O is as follows:

$$U_O = \begin{cases} \frac{1}{2}\eta\left(\frac{1}{\rho} - \frac{1}{\rho_O}\right)^2 & if\ \rho \le \rho_O \\ 0 & if\ \rho > \rho_O \end{cases} \tag{7}$$

where η is the repulsive potential constant, ρ is the closest distance between the robot and the obstacle, and ρ_O is the distance limit of the potential field influence.

The Khatib's attractive APF force equation is written as:

$$F_O = \begin{cases} \eta\left(\frac{1}{\rho} - \frac{1}{\rho_O}\right)\frac{1}{\rho^2}\frac{\delta\rho}{\delta x} & if\ \rho \le \rho_O \\ 0 & if\ \rho > \rho_O \end{cases} \tag{8}$$

where $\frac{\delta\rho}{\delta x}$ represents the partial derivative vector of the distance between the robot and the obstacle.

The APF force equation is the sum of attractive APF and repulsive APF forces written as follows:

$$F_{art} = F_{x_d} + \sum_{i=1}^{n} F_{O,i} \tag{9}$$

III. Local Minima

Local minima is an area where the value of the attractive force is the same as that of the repulsive force generating zero value of the resultant force meaning that the area does not have force value and making the robot unable to move [16] as shown on Fig. 2. Several previous researchers have studied and modified the potential field force to avoid local minima such as the wall-fallowing algorithm applied by Xiaoping Yun & Ko-Cheng Tan to modify the potential field algorithm so that the robot can avoid local minima [6].

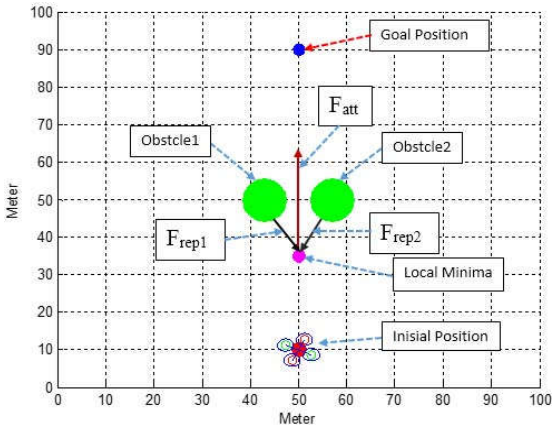

Fig. 2. Area with loca minima

IV. Modified Potential Field

The potential field algorithm on attractive APF U_{att} is formulated as:

$$U_{att}\left(x,y\right) = \frac{1}{2} K_a \left[\left(x - x_\Gamma\right)^2 + \left(y - y_\Gamma\right)^2\right] \tag{10}$$

where K_a is the amplifier parameter and $\left(x_\Gamma, y_\Gamma\right)$ is the goal position value. Based on equation (10), the attractive APF force equation is written as:

$$\begin{aligned} F_{att\_x}\left(x,y\right) &= -\frac{\partial U_{att}\left(x,y\right)}{\partial x}, \\ F_{att\_x}\left(x,y\right) &= -K_a\left(x_t - x_d\right) \end{aligned} \tag{11}$$

and:

$$\begin{aligned} F_{att\_y}\left(x,y\right) &= -\frac{\partial U_{att}\left(x,y\right)}{\partial y}, \\ F_{att\_y}\left(x,y\right) &= -K_a\left(y_t - y_d\right) \end{aligned} \tag{12}$$

The following equation is the mathematic model for the potential field algorithm in Repulsive APF:

$$U_{rep} = \frac{K_r}{\sqrt{\left(x - x_O\right)^2 + \left(y - y_O\right)^2}} \tag{13}$$

Based on equation (13), the Repulsive APF equation is as the following:

$$\begin{aligned} F_{rep\_x}\left(x,y\right) &= -\frac{\partial U_{rep}\left(x,y\right)}{\partial x}, \\ F_{rep\_x}\left(x,y\right) &= \frac{-K_r\left(x_t - x_O\right)}{\sqrt{\left(\left(x_t - x_O\right)^2 + \left(y_t - y_O\right)^2\right)^3}} \end{aligned} \tag{14}$$

and:

$$F_{rep\_y}(x,y) = -\frac{\partial U_{rep}(x,y)}{\partial y},$$
$$F_{rep\_y}(x,y) = \frac{-K_r(y_t - y_O)}{\sqrt{\left((x_t - x_O)^2 + (y_t - y_O)^2\right)^3}} \quad (15)$$

The APF force equation on the x-axis is written as:

$$F_{art\_x}(x,y) = F_{att\_x}(x,y) + \sum_{i=1}^{n} F_{rep\_x,i}(x,y),$$
$$F_{art\_x}(x,y) = -K_a(x_t - x_d) + \quad (16)$$
$$+ \frac{K_r(x_t - x_O)}{\sqrt{\left((x_t - x_O)^2 + (y_t - y_O)^2\right)^3}}$$

On the y-axis it is written as:

$$F_{art\_y}(x,y) = F_{att\_y}(x,y) + \sum_{i=1}^{n} F_{rep\_y,i}(x,y),$$
$$F_{art\_y}(x,y) = -K_a|y_t - y_d| + \quad (17)$$
$$+ \frac{K_r|y_t - y_O|}{\sqrt{\left[(x_t - x_O)^2 + (y_t - y_O)^2\right]^3}}$$

Based on equations (15) and (16) the resultant APF force is obtained as formulated below:

$$F_{art} = \sqrt{\begin{matrix} F_{art\_x}(x,y)^2 + F_{art\_y}(x,y)^2 + \\ +2F_{art\_x}(x,y)F_{art\_y}(x,y)\cos\psi \end{matrix}} \quad (18)$$

where ψ is an angle formed by $F_{art\_x}(x,y)$ and $F_{art\_y}(x,y)$:

$$\psi = \arctan\left(\frac{F_{art}(y)}{F_{art}(x)}\right) \quad (19)$$

In this study a virtual obstacle was used to remove local minima by placing a virtual obstacle between two real obstacles as shown in Fig. 3.

It is seen that the virtual obstacle has a circle shape located between the two real obstacles. The virtual obstacle's diameter is the distance between the two real obstacles.

With the virtual obstacle, there are three repulsive forces: one virtual obstacle repulsive force and two real obstacles repulsive forces.

Based on the explanation above, the potential field algorithm on repulsive APF U_{rep_x} of x-axis is modified as follows:

$$U_{rep\_x\_1}(x,y) = \begin{cases} \dfrac{K_r}{\sqrt{(x_t - x_{O1})^2 + (y_t - y_{O1})^2}} & \text{if } x_t \le d_O \\ 0 & \text{if } x_t > d_O \end{cases} \quad (20)$$

$$U_{rep\_x\_2}(x,y) = \begin{cases} \dfrac{K_r}{\sqrt{(x_t - x_{O2})^2 + (y_t - y_{O2})^2}} & \text{if } x_t \le d_O \\ 0 & \text{if } x_t > d_O \end{cases} \quad (21)$$

$$U_{rep\_x\_v}(x,y) = \begin{cases} \dfrac{K_r}{\sqrt{(x_t - x_{Ov})^2 + (y_t - y_{Ov})^2}} & \text{if } x_t \le d_O \\ 0 & \text{if } x_t > d_O \end{cases} \quad (22)$$

The potential field algorithm on repulsive APF U_{rep_y} of y axis is modified as follows:

$$U_{rep\_y\_1}(x,y) = \begin{cases} \dfrac{K_r}{\sqrt{(x_{lt} - x_{O1})^2 + (y_{lt} - y_{O1})^2}} & \text{if } y_{lt} \le d_O \\ 0 & \text{if } y_{lt} > d_O \end{cases} \quad (23)$$

$$U_{rep\_y\_2}(x,y) = \begin{cases} \dfrac{K_r}{\sqrt{(x_{lt} - x_{O2})^2 + (y_{lt} - y_{O2})^2}} & \text{if } y_{lt} \le d_O \\ 0 & \text{if } y_{lt} > d_O \end{cases} \quad (24)$$

$$U_{rep\_y\_v}(x,y) = \begin{cases} \dfrac{K_r}{\sqrt{(x_{lt} - x_{Ov})^2 + (y_{lt} - y_{Ov})^2}} & \text{if } y_{lt} \le d_O \\ 0 & \text{if } y_{lt} > d_O \end{cases} \quad (25)$$

The following is the repulsive APF equation of x-axis derived from the modification:

$$F_{rep\_x\_1}(x,y) = \begin{cases} \dfrac{K_r(x_t - x_{O1})}{\sqrt{\left((x_t - x_{O1})^2 + (y_t - y_{O1})^2\right)^3}} & \text{if } x_t \le d_{O1} \\ 0 & \text{if } x_t > d_{O1} \end{cases} \quad (26)$$

$$F_{rep\_x\_2}(x,y)=\begin{cases}\dfrac{K_r\left(x_{lt}-x_{O2}\right)}{\sqrt{\left(\left(x_{lt}-x_{O2}\right)^2+\left(y_{lt}-y_{O2}\right)^2\right)^3}} & \text{if } x_{lt}\le d_{O2}\\ 0 & \text{if } x_{lt}>d_{O2}\end{cases} \quad (27)$$

$$F_{rep\_x\_v}(x,y)=\begin{cases}\dfrac{K_r\left(x_{lt}-x_{Ov}\right)}{\sqrt{\left(\left(x_{lt}-x_{Ov}\right)^2+\left(y_{lt}-y_{Ov}\right)^2\right)^3}} & \text{if } x_{lt}\le d_{Ov}\\ 0 & \text{if } x_{lt}>d_{Ov}\end{cases} \quad (28)$$

while the repulsive APF equation of y-axis is as follows:

$$F_{rep\_y\_1}(x,y)=\begin{cases}\dfrac{K_r\left(y_t-y_{O1}\right)}{\sqrt{\left(\left(x_t-x_{O1}\right)^2+\left(y_t-y_{O1}\right)^2\right)^3}} & \text{if } x_t\le d_{O1}\\ 0 & \text{if } x_t>d_{O1}\end{cases} \quad (29)$$

$$F_{rep\_x\_2}(x,y)=\begin{cases}\dfrac{K_r\left(y_{lt}-y_{O2}\right)}{\sqrt{\left(\left(x_{lt}-x_{O2}\right)^2+\left(y_{lt}-y_{O2}\right)^2\right)^3}} & \text{if } x_{lt}\le d_{O}\\ 0 & \text{if } x_{lt}>d_{O}\end{cases} \quad (30)$$

$$F_{rep\_x\_v}(x,y)=\begin{cases}\dfrac{K_r\left(y_t-y_{Ov}\right)}{\sqrt{\left(\left(x_{lt}-x_{Ov}\right)^2+\left(y_{lt}-y_{Ov}\right)^2\right)^3}} & \text{if } x_{lt}\le d_{O}\\ 0 & \text{if } x_{lt}>d_{O}\end{cases} \quad (31)$$

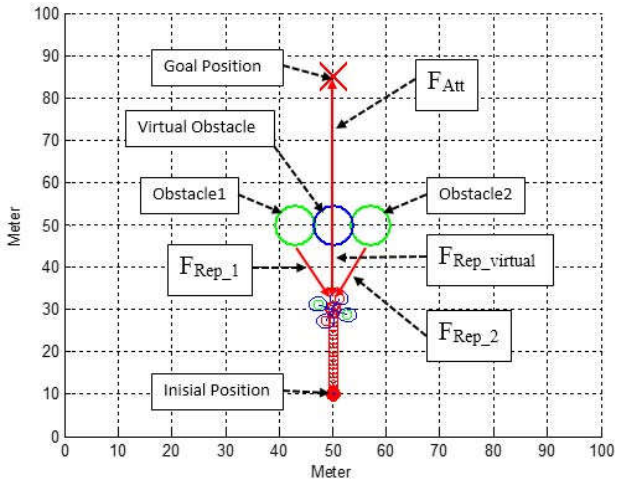

Fig. 3. Method of avoiding local minima with a virtual obstacle

The virtual obstacle method is applied if the distance between two real obstacles is smaller than the robot wide, because, if the distance between two real obstacles is bigger than the robot wide, the robot will be able to pass through the obstacles.

V. Quadrotor Modeling

A quadrotor is one of the UAV types with rotary-wing similar to a helicopter [17]-[19], [23]-[25]. The difference between quadrotor and helicopter is in the control system [20].

The control system in the helicopter merely controls a single motor and angle on the propeller, while in the quadrotor it controls four motors. The quadrotor model based on Corke model [21] is shown in Fig. 4.

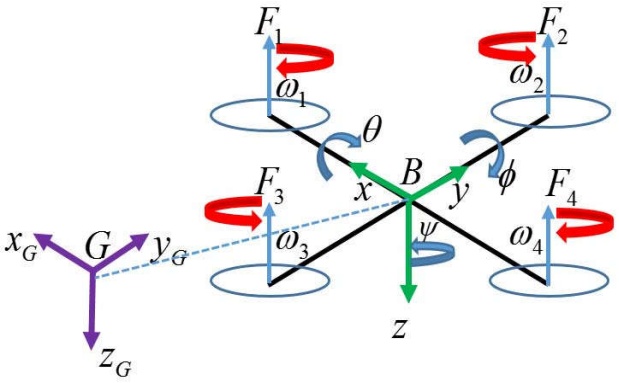

Fig. 4. Quadrotor Modeling

Figure 4 shows that G is the global frame with (x_G, y_G, z_G) coordinates used as the fixed reference frame of the system.

While B is the quadrotor frame with (x, y, z) coordinates that have four rotors at the end of the arm, each frame consists of a pair of rotors in which each rotor rotates in the same direction. The frame of quadrotor B rotating around x_G, y_G, and z_G axes, has three Euler angular transformations.

The frame of quadrotor B rotating around z_G axis (yaw) has an Euler angular rotation transformation $R_{z_G}(\psi)$, the frame of quadrotor B rotating around x_G axis (pitch) has an Euler angular rotation transformation $R_{x_G}(\theta)$, and the frame of quadrotor B rotating around y_G axis (roll) has an Euler angular rotation transformation $R_{y_G}(\varphi)$.

By substituting the newton's second law into the forces of the quadrotor, the acceleration of x, y and z axes are obtained as written in the following equations [22]:

$$\ddot{x}=-\frac{1}{m}T\left(\cos\varphi\sin\theta\cos\psi+\sin\varphi\sin\psi\right)-\left(\dot{\theta}\dot{z}-\dot{\psi}\dot{y}\right) \quad (32)$$

$$\ddot{y} = -\frac{1}{m}T\left(\cos\varphi\sin\theta\sin\psi - \sin\varphi\cos\psi\right) - \left(\dot{\theta}\dot{x} - \dot{\varphi}\dot{z}\right) \quad (33)$$

$$\ddot{z} = mg - \frac{1}{m}T\left(\cos\varphi\cos\theta\right) - \left(\dot{\varphi}\dot{y} - \dot{\theta}\dot{x}\right) \quad (34)$$

The angular acceleration equation of the quadrotor is obtained as follows:

$$\ddot{\varphi} = \frac{db}{\mathrm{I}_x}\left(\omega_4^2 - \omega_2^2\right) - \frac{\mathrm{I}_z - \mathrm{I}_y}{\mathrm{I}_x}\dot{\theta}\dot{\psi} \quad (35)$$

$$\ddot{\theta} = \frac{db}{\mathrm{I}_y}\left(\omega_1^2 - \omega_3^2\right) - \frac{\mathrm{I}_x - \mathrm{I}_z}{\mathrm{I}_y}\dot{\varphi}\dot{\psi} \quad (36)$$

$$\ddot{\psi} = \frac{k}{\mathrm{I}_x}\left(\omega_1^2 - \omega_2^2 + \omega_3^2 - \omega_4^2\right) - \frac{\mathrm{I}_y - \mathrm{I}_x}{\mathrm{I}_z}\dot{\varphi}\dot{\theta} \quad (37)$$

VI. Proposed Path Planning

Applying APF force to the quadrotor was the first problem in this research.

Based on 12 non-linear equations, a quadrotor is a Multiple Input Multiple Output (MIMO) system which is an under-actuated system with four inputs of motor rotation speeds defined as ω_i with $i = 1,2,3,4$ and six outputs of $[x, y, z, \varphi, \theta, \psi]$.

The equation of the acceleration of x and y is as follows:

$$\ddot{x} = \frac{U_x}{m} \quad (38)$$

$$\ddot{y} = \frac{U_y}{m} \quad (39)$$

Based on the problem, equations (38) and (39) in the APF force of the x, y-axes combined with the force of the x and y axes equations is formulated as follows:

$$U_x = F_{art\_x}(x, y) \quad (40)$$

$$U_y = F_{art\_y}(x, y) \quad (41)$$

Equations (40) and (41) are applied to the area without obstacles, so that the speed equations on the x-axis are:

$$\tau_x = -K_a\left(x_t - x_d\right) \quad (42)$$

$$\tau_y = -K_a\left(y_t - y_d\right) \quad (43)$$

When the goal position (x_d, y_d) is far from the robot position (x_t, y_t) as shown in Fig. 5, the magnitude torque force of τ_x and τ_y leads to unstable quadrotor due to the large angles of the roll and pitch.

The figure shows that (x_d, y_d) is the goal position, (x_t, y_t) is the position of the robot, and d_l is the closest distance to the goal position. Referring to the problems previously mentiones, the potential field algorithm on Attractive APF U_{att} x-axis is modified as:

$$U_{att\_x}(x, y) = \begin{cases} \frac{1}{2}K_a\left(x_t - x_d\right)^2 & if\ x_t \le x_d + d_l \\ K_a d_l\left(x_t - x_d\right) & if\ x_t > x_d + d_l \end{cases} \quad (44)$$

and the potential field algorithm on Attractive APF U_{att} y-axis is modified as:

$$U_{att\_y}(x, y) = \begin{cases} \frac{1}{2}K_a\left(y_t - y_d\right)^2 & if\ y_t \le y_d + d_l \\ K_a d_l\left(y_t - y_d\right) & if\ y_t > y_d + d_l \end{cases} \quad (45)$$

Based on the modification, the Attractive APF force equation of x axis is formulated as:

$$F_{att\_x}(x, y) = \begin{cases} -K_a\left|x_t - x_d\right| & if\ x_t \le x_d + d_l \\ K_a d_l & f\ x_t > x_d + d_l \end{cases} \quad (46)$$

The Attractive APF on x axis has the following equation:

$$F_{att\_x}(x, y) = \begin{cases} -K_a\left|x_t - x_d\right| & if\ x_t \le x_d + d_l \\ K_a d_l & f\ x_t > x_d + d_l \end{cases} \quad (47)$$

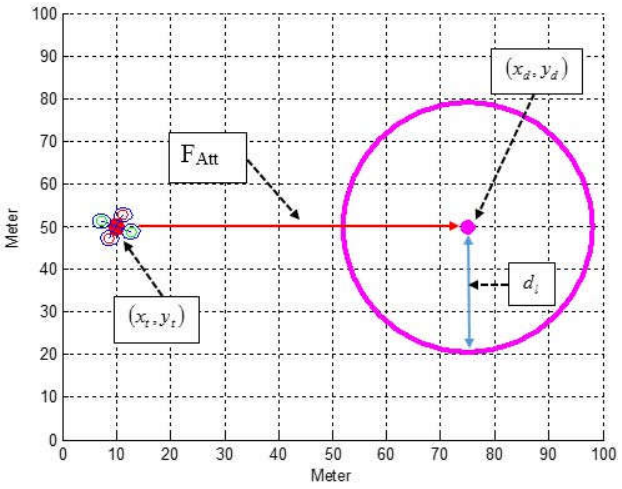

Fig. 5. Potential field attractive model

Equations (46) and (47) were applied to the area with obstacles and far from the destination position.

The torque force equation on the x,y-axis is:

$$\tau_x = K_r \frac{(x_t - x_O)}{\sqrt{\left((x_t - x_O)^2 + (y_t - y_O)^2\right)^3}} \quad (48)$$

$$\tau_y = K_r \frac{(y_t - y_O)}{\sqrt{\left[(x_t - x_O)^2 + (y_t - y_O)^2\right]^3}} \quad (49)$$

When the obstacle position is close to the robot position as it is shown in Fig. 6, the speed of $\ddot{x}$ and $\ddot{y}$ is increasing leading to an unstable quadrotor while avoiding obstacles due to the large angles of the roll and pitch. It is seen in Fig. 6 that (x_O, y_O) is the obstacle position, (x_t, y_t) is the robot position, and d_O is the safest distance to avoid obstacles.

With these problems the potential field algorithm on Repulsive APF x axis U_{rep_x} is modified as:

$$U_{rep\_x}(x,y) = \begin{cases} \dfrac{K_r}{\sqrt{(x_t - x_O)^2 + (y_t - y_O)^2}} & \text{if } x_t \le d_O \\ 0 & \text{if } x_t > d_O \end{cases} \quad (50)$$

and the potential field algorithm on Repulsive APF U_{att} y axis is modified as:

$$U_{rep\_y}(x,y) = \begin{cases} \dfrac{K_r}{\sqrt{(x_t - x_O)^2 + (y_t - y_O)^2}} & \text{if } y_t \le d_O \\ 0 & \text{if } y_t > d_O \end{cases} \quad (51)$$

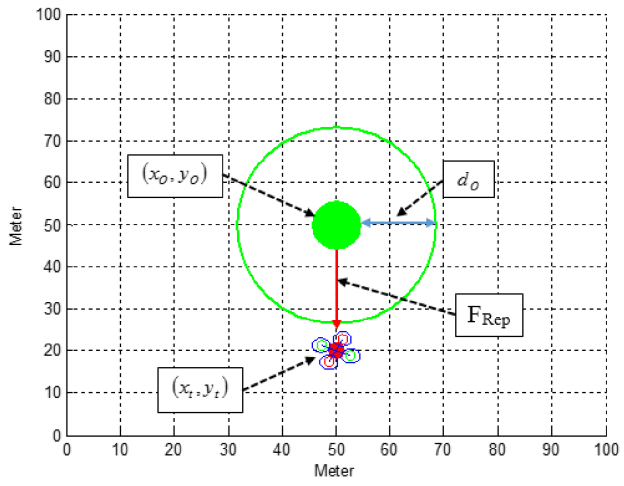

Fig. 6. Potential field repulsive algorithm model

Based on the modification the APF force equation of x axis is written as follows:

$$F_{rep\_x}(x,y) = \begin{cases} \dfrac{K_r (x_t - x_O)}{\sqrt{\left((x_t - x_O)^2 + (y_t - y_O)^2\right)^3}} & \text{if } x_t \le d_O \\ 0 & \text{if } x_t > d_O \end{cases} \quad (52)$$

The Repulsive APF on y axis is written as the following equation:

$$F_{rep\_y}(x,y) = \begin{cases} \dfrac{K_r (y_t - y_O)}{\sqrt{\left((x_t - x_O)^2 + (y_t - y_O)^2\right)^3}} & \text{if } y_t \le d_O \\ 0 & \text{if } y_t > d_O \end{cases} \quad (53)$$

VII. Results and Analysis

In the experiment, the potential algorithm was tested.

The test was using virtual obstacle created by two adjacent obstacles applied to a quadrotor to avoid local minima by using two software of ROS (robot operating system) and Matlab.

Matlab was used to create a design potential field algorithm modification by creating a virtual obstacle and to model the quadrotor. The algorithm was simulated to see the performance of the quadrotor when moving to the goal position and avoiding the local minima in an unknown area model.

The potential field algorithm was first tested by comparing modified algorithm using a virtual obstacle and Zhu et al.'s [17] potential field algorithm in an unknown area that contained two static obstacles as shown in Figs. 7.

It shows that the quadrotor is placed at the initial position (10, 50), and the goal position (50, 95). The static obstacles are located at the position (43, 50) and (57, 50). There is a local minima formed between two obstacles that cause the quadrotor to stop in the area. Fig. 7(a) shows that the quadrotor tested by using Khatib's potential field algorithm indicated in red color stops at local minima.

Zhu et al.'s potential field algorithm indicated in blue color shows that the quadrotor is able to avoid local minima because the area generating local minima is closed by using a virtual obstacle formed by several internal agents.

Fig. 7(b) shows that the quadrotor tested by using Khatib's potential field algorithm indicated in red color stops at local minima but by using the potential field algorithm proposed by the author indicated in blue, the quadrotor can avoid local minima because the area generating local minima is closed by using a virtual obstacle which its diameter has the same length as the distance between the two obstacles. The second test for the second experiment was conducted by shifting the

distance between the two obstacles as shown in Figs. 8.

It shows that the two static obstacles are located at the position (42, 50) and (58, 50). Fig. 8(a) shows that the quadrotor is tested by using Khatib's potential field algorithm indicated in red color and the Zhu et al.'s potential field algorithm indicated in blue color. The test shows that there is still loca minima causing the robot to stop.

Fig. 8(b) shows Khatib's potential field algorithm indicated in red color, and the proposed algorithm created is indicated in blue color. By using the proposed algorithm, the quadrotor avoids local minima because the area generating local minima was closed by using a virtual obstacle. The third experiment is conducted by shifting the distance between the two obstacles as shown in Fig. 9.The picture shows that the two static obstacles are at the position (41, 50) and (59, 50).

The quadrotor was tested by using Khatib's potential field, Zhu et al.'s and the proposed algorithm and it showed that it is able to avoid the obstacles because there are no loca minima generated.

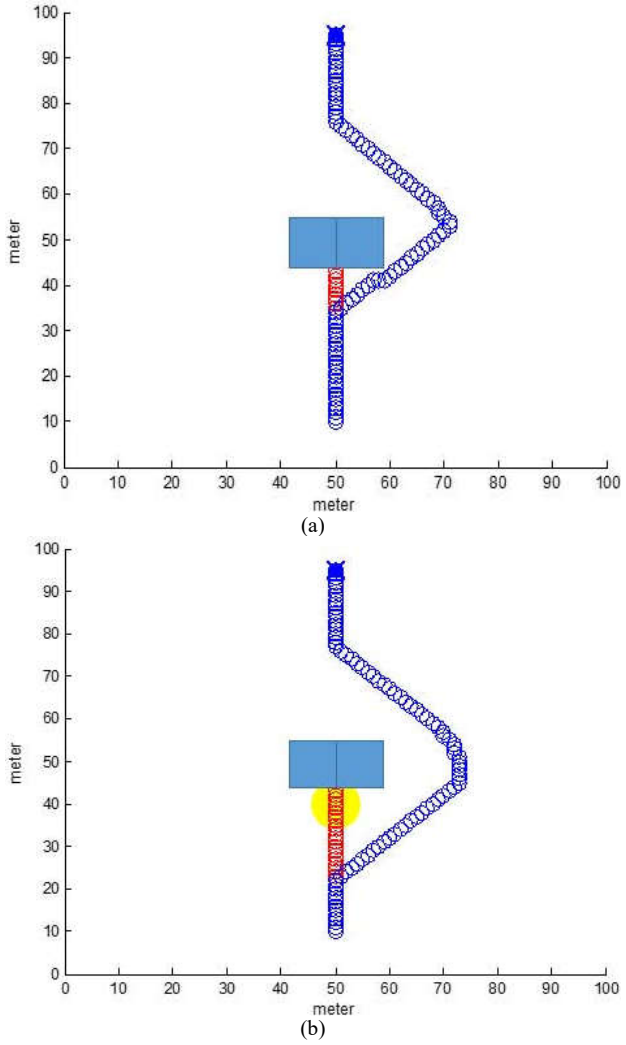

Figs. 7. The first test of (a) Zhu et al.'s algorithm (Zhu et al. 2008) (b) and the proposed algorithm

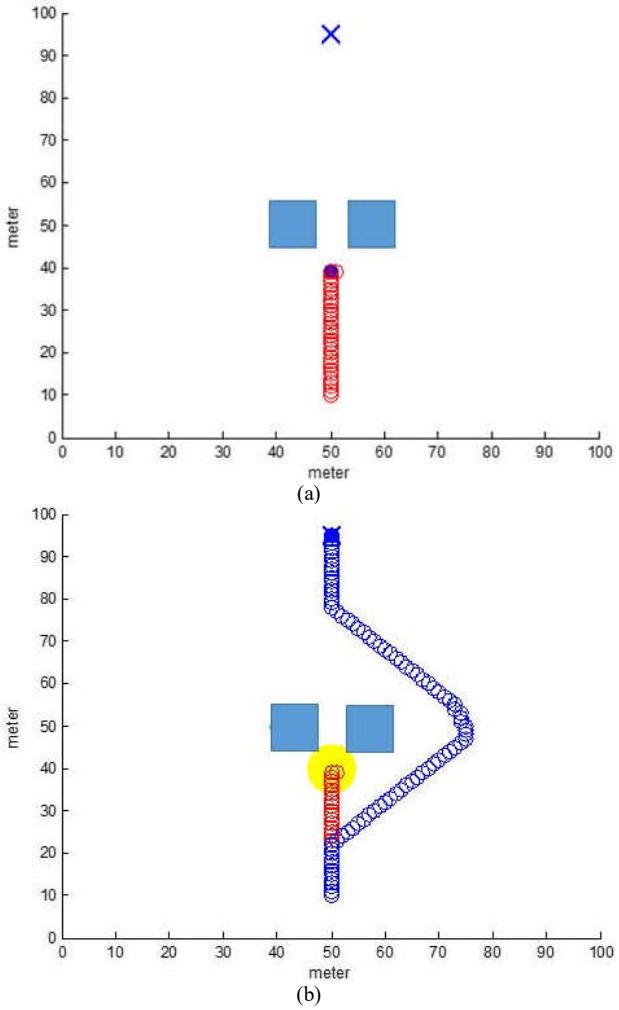

Figs. 8. The second test (a) Zhu et al.'salgorithm (Zhu et al. 2008) (b) the author's algorithm

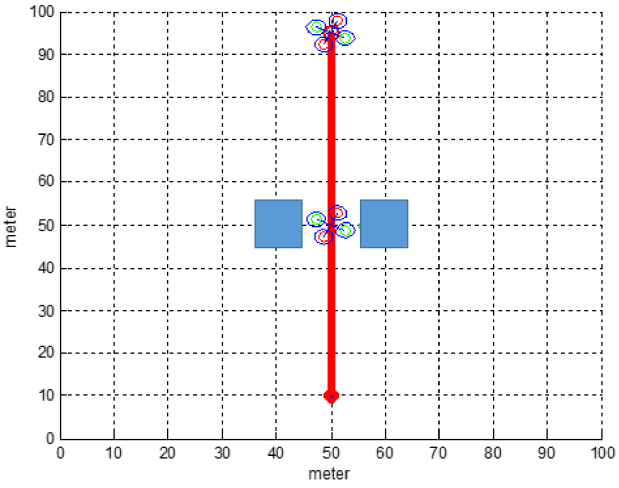

Fig. 9. The third test using two obstacles

VIII. Conclusion

The research creates a virtual obstacle placed between two real obstacles to prevent loca minima generated from the zero value of the attractive and repulsive force. The

diameter of the virtual obstacle is the distance between the two obstacles so that there are no gaps in between the virtual obstacle and the real obstacles to prevent the creation of local minima. The proposed algorithm adds a repulsive force of the virtual obstacle so that the total value of the forces of the obstacles is not equal to zero which means that there is no local minima enabling the robot avoid the obstacles.

Acknowledgements

This research was supported by Doctoral Project Grant from DIKTI through Research Directorate, Universitas Muhammadiyah Yogyakarta with the contract number: 047/HB-LIT/IV/2017, awarded to A/P Iswanto, S.T., M.Eng.

References

[1] O. Khatib, Real time obstacle avoidance for manipulators and mobile robots, *International Journal of Robotics and Research*, vol. 5, no. 1. pp. 90–98, 1986.

[2] B. Faverjon and P. Tournassoud, A local based approach for path planning of manipulators with a high number of degrees of freedom, in *Proceedings. 1987 IEEE International Conference on Robotics and Automation*, 1987, pp. 1152–1159.

[3] C. W. Warren, Global path planning using artificial potential fields, in *Proceedings, 1989 International Conference on Robotics and Automation*, 1989, pp. 316–321.

[4] C. I. Connolly, J. B. Burns, and R. Weiss, Path planning using Laplace's equation, in *Proceedings., IEEE International Conference on Robotics and Automation*, 1990, pp. 2102–2106.

[5] J. Barraquand, B. Langlois, and J.-C. Latombe, Numerical potential field techniques for robot path planning, *IEEE Trans. Syst. Man. Cybern.*, vol. 22, no. 2, pp. 224–241, 1992.

[6] Xiaoping Yun and Ko-Cheng Tan, A wall-following method for escaping local minima in potential field based motion planning, in *1997 8th International Conference on Advanced Robotics. Proceedings. ICAR'97*, 1997, pp. 421–426.

[7] W. Newman and N. Hogan, High speed robot control and obstacle avoidance using dynamic potential functions, in *Proceedings. 1987 IEEE International Conference on Robotics and Automation*, 1987, pp. 14–24.

[8] J. Kim and P. K. Khosla, Real-time obstacle avoidance using harmonic potential functions, *IEEE Trans. Robot. Autom.*, vol. 8, no. 3, pp. 338–349, 1992.

[9] J. Borenstein and Y. Koren, Real-time obstacle avoidance for fast mobile robots, *IEEE Trans. Syst. Man. Cybern.*, vol. 19, no. 5, pp. 1179–1187, Sep. 1989.

[10] R. Spence and S. Hutchinson, Dealing With Unexpected Moving Obstacles By Integrating Potential Field Planning With Inverse Dynamics Control, in *Proceedings of the IEEE/RSJ International Conference on Intelligent Robots and Systems*, 1992, vol. 3, pp. 1485–1490.

[11] S. Sundar and Z. Shiller, Optimal obstacle avoidance based on the Hamilton-Jacobi-Bellman equation, in *Proceedings of the 1994 IEEE International Conference on Robotics and Automation*, 1994, pp. 2424–2429.

[12] A. A. Masoud, S. A. Masoud, and M. M. Bayoumi, Robot navigation using a pressure generated mechanical stress field: 'the biharmonic potential approach, in *Proceedings of the 1994 IEEE International Conference on Robotics and Automation*, 1994, pp. 124–129.

[13] G. Dozier, A. Homaifar, S. Bryson, and L. Moore, Artificial potential field based robot navigation, dynamic constrained optimization and simple genetic hill-climbing, in *1998 IEEE International Conference on Evolutionary Computation Proceedings. IEEE World Congress on Computational Intelligence* (Cat. No.98TH8360), 1998, pp. 189–194.

[14] Y. Zhu, T. Zhang, and J. Song, An improved wall following method for escaping from local minimum in artificial potential field based path planning, in *Proceedings of the 48h IEEE Conference on Decision and Control (CDC) held jointly with 2009 28th Chinese Control Conference*, 2009, pp. 6017–6022.

[15] I. Iswanto, O. Wahyunggoro, and A. I. Cahyadi, Formation Pattern Based on Modified Cell Decomposition Algorithm, *Int. J. Adv. Sci. Eng. Inf. Technol.*, vol. 7, no. 3, pp. 829–835, 2017.

[16] H. Noborio, S. Wazumi, S. Fukuda, and S. Arimoto, A Potential Approach For A Point Mobile Robot On An Implicit Potential Field Without The Generation Of Local Minima, in *Proceedings. IEEE/RSJ International Workshop on Intelligent Robots and Systems' (IROS '89) The Autonomous Mobile Robots and Its Applications*, 1989, pp. 70–77.

[17] Iswanto, I., Ataka, A., Inovan, R., Wahyunggoro, O., Imam Cahyadi, A., Disturbance Rejection for Quadrotor Attitude Control Based on PD and Fuzzy Logic Algorithm, (2016) *International Review of Automatic Control (IREACO)*, 9 (6), pp. 405-412. doi: https://doi.org/10.15866/ireaco.v9i6.9930

[18] Agustinah, T., Isdaryani, F., Nuh, M., Tracking Control of Quadrotor Using Static Output Feedback with Modified Command-Generator Tracker, (2016) *International Review of Automatic Control (IREACO)*, 9 (4), pp. 242-251. doi: https://doi.org/10.15866/ireaco.v9i4.9431

[19] Krafes, S., Chalh, Z., Saka, A., Visual Servoing of a Spherical Inverted Pendulum on a Quadrotor Using Backstepping Controller, (2018) *International Review of Aerospace Engineering (IREASE)*, 11 (1), pp. 6-14. doi: https://doi.org/10.15866/irease.v11i1.13460

[20] R. Mahony, V. Kumar, and P. Corke, Multirotor Aerial Vehicles: Modeling, Estimation, and Control of Quadrotor, *IEEE Robot. Autom. Mag.*, vol. 19, no. 3, pp. 20–32, Sep. 2012.

[21] Iswanto, O. Wahyunggoro, and A. I. Cahyadi, Hover position of quadrotor based on PD-like fuzzy linear programming *Int. J. Electr. Comput. Eng.*, vol. 6, no. 5, pp. 2251–2261, 2016.

[22] N. Maharani Raharja, E. Firmansyah, A. Imam Cahyadi, and I. Iswanto, Hovering Control of Quadrotor Based on Fuzzy Logic, *Int. J. Power Electron. Drive Syst.*, vol. 8, no. 1, p. 492, Mar. 2017.

[23] Manzoor, M., Maqsood, A., Hasan, A., Quadratic Optimal Control of Aerodynamic Vectored UAV at High Angle of Attack, (2016) *International Review of Aerospace Engineering (IREASE)*, 9 (3), pp. 70-79. doi:https://doi.org/10.15866/irease.v9i3.8119

[24] Aziz, M., Elsayed, A., CFD Investigations for UAV and MAV Low Speed Airfoils Characteristics, (2015) *International Review of Aerospace Engineering (IREASE)*, 8 (3), pp. 95-100. doi:https://doi.org/10.15866/irease.v8i3.6212

[25] Carloni, G., Bousson, K., A Nonlinear Control Method for Autonomous Navigation Guidance, (2016) *International Review of Civil Engineering (IRECE)*, 7 (4), pp. 102-113. doi:https://doi.org/10.15866/irece.v7i4.10757

Authors' information

Iswanto was born in Sleman, Yogyakarta, Indonesia, in 1981. He received the B.S degree and M.Eng degree from Universitas Gadjah Mada, Yogyakarta, Indonesia in 2007 and 2009. Now, he is on Phd Program at Universitas Gadjah Mada. He has been a Lecturer and Researcher in the Electrical Engineering Department at Universitas Muhammadiyah Yogyakarta since 2010. His current research is focused on formation control, path planning and Control UAV.